Algebraic Instability of Hollow Electron Columns and Cylindrical Vortices

Ralph A. Smith
Department of Physics, B-019, University of California, San Diego, La Jolla, California 92093

Marshall N. Rosenbluth
Department of Physics, B-019, University of California, San Diego, La Jolla, California 92093
and G. A. Technologies, La Jolla, California 92138
(Received 23 October 1989)

An axisymmetric, magnetically confined electron column, in which the $\mathbf{E}\times\mathbf{B}$ rotation frequency is not a monotone function of radius, is linearly unstable to two-dimensional, electrostatic disturbances with azimuthal mode number $l=1$. The perturbation density is asymptotically proportional to $\sqrt{t}$ and may be described as a shift of the core of the column. A particle-in-cell simulation indicates that harmonics grow rapidly and that there are secondary instabilities. An identical instability arises in hollow circular vortex columns in an inviscid, incompressible neutral fluid.

PACS numbers: 52.25.Wz, 47.20.Ft, 52.35.Py

Shear-flow or diocotron instabilities often arise in low-density non-neutral plasmas; here we explore a new and unusual case. We consider an axisymmetric single-species plasma confined by a magnetic field $B\hat{z}$ which is sufficiently strong to justify a guiding-center drift approximation. Such a plasma has been studied extensively in laboratory experiments (see, e.g., Ref. 1). If the radial density profile is hollow, so that the $\mathbf{E}\times\mathbf{B}$ rotation frequency has a stationary point as a function of radius, we find a new, algebraically growing instability, associated with the continuous spectrum of the $\mathbf{E}\times\mathbf{B}$ evolution operator. This situation may be contrasted with more familiar, exponentially growing diocotron instabilities, and occurs even in the absence of the latter. We have observed the algebraic growth of the instability in particle simulations, which also illustrate unusual features of its large-amplitude behavior.

The cross-field evolution of the guiding-center density is described by the continuity equation $(\partial/\partial t+\mathbf{v}_E\cdot\nabla)n=0$, where the $\mathbf{E}\times\mathbf{B}$ velocity is $\mathbf{v}_E=cB^{-1}\hat{z}\times\nabla\phi$, and the electrostatic potential ϕ is related to n by the Poisson equation $\nabla^2\phi=4\pi en$. Cylindrical polar coordinates (r,θ,z) are used here. These equations are identical, up to constants of proportionality, to the vorticity–stream-function formulation of the Euler equations describing the flow of an inviscid, two-dimensional neutral fluid of uniform density. The vorticity is identified with the electron density n, and the stream function, with the electrostatic potential ϕ.

Let the equilibrium be described by a smooth density $n_0(r)$ which is independent of z and θ, with a conducting wall located at $r=R$, where $\phi=0$. Hollow profiles like the one shown in Fig. 1 will be of special interest. Similar electron columns have been created in the laboratory.[2] We allow for electrostatic perturbations which vary in r and θ.

A corollary of Rayleigh's inflection-point theorem,[3] as extended by Arnol'd,[4] shows that such an equilibrium is nonlinearly stable if n_0 is monotone in r. We derive a sufficient condition for instability which is somewhat more restrictive than those previously available.

Since the equilibrium is axisymmetric, linear stability may be analyzed independently for each azimuthal Fourier component; the new instability involves only the fundamental modes. We isolate an infinitesimal perturbation potential $\delta\phi=\phi_1(r,t)e^{i\theta}+\text{c.c.}$ The continuity equation may be written as

$$\left(\frac{\partial}{\partial t}+i\omega_E(r)\right)\left(\frac{1}{r}\frac{\partial}{\partial r}r\frac{\partial}{\partial r}-\frac{1}{r^2}\right)\phi_1 - i\frac{4\pi ec}{Br}n_0'(r)\phi_1=0, \quad (1)$$

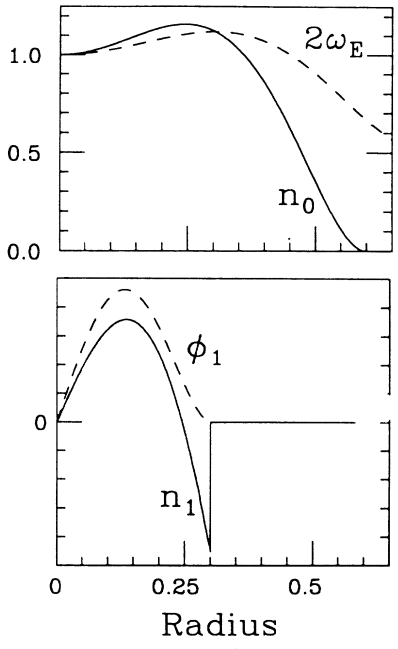

FIG. 1. Top: radial density (or vorticity) and rotation-frequency profiles of the fluid equilibrium used in the simulation. The boundary condition $\phi=0$ is imposed at $r=1$. Bottom: Asymptotic radial dependence of density (vorticity) and potential amplitudes for a typical $l=1$ perturbation. Phases are independent of r.

where

$$\omega_E(r) = (2\pi ce/Br^2)\int_0^r dr\, r n_0(r)$$

is the equilibrium rotation frequency. Note that monotonicity of $n_0(r)$ implies monotonicity of $\omega_E(r)$.

A conventional normal-mode analysis[5] shows that there is a single smooth eigenfunction—the fundamental diocotron mode—with a purely real frequency, equal to the $\mathbf{E}\times\mathbf{B}$ rotation frequency at the wall, if dn_0/dr vanishes at $r=R$. For $l \geq 2$, there may be diocotron instabilities which grow exponentially in time if $\omega_E(r)$ is sufficiently peaked away from the origin. Numerical calculations have shown that certain smooth, hollow equilibria are not afflicted by such exponentially growing instabilities (e.g., those close to the stable step-function profiles described by Levy[6]). The stability of the system in this case is said to be spectrally indeterminate.

In addition to any normal modes, temporal evolution of a perturbation generally involves contributions from the continuous spectrum of the operator acting on ϕ_1 in Eq. (1), corresponding to the range of values of $\omega_E(r)$. These may be examined by consideration of the initial-value problem, following Case.[7] In terms of a Laplace transform $\phi_p(r) = \int_0^\infty dt\, e^{-pt}\phi_1(r,t)$, where the real part of p is sufficiently large to insure convergence, Eq. (1) becomes

$$[p+i\omega_E(r)]\left(\frac{1}{r}\frac{\partial}{\partial r}r\frac{\partial}{\partial r}-\frac{1}{r^2}\right)\phi_p - i\frac{4\pi ec}{Br}\frac{dn_0}{dr}\phi_p = 4\pi e n_1(r,0)\,, \tag{2}$$

where $n_1(r,0)e^{il\theta}$ is the density perturbation imposed at $t=0$. It can be shown that contributions from the continuous spectrum to perturbation potentials proportional to $e^{il\theta}$ with $l \geq 2$ decay algebraically in time.[7,8] No such argument applies to the $l=1$ component, because of a degeneracy in the fundamental solution for Eq. (2). The initial-value problem may be reduced to quadratures as follows.[9] Noting that

$$\frac{\partial}{\partial r}r^3(p+i\omega_E)^2\frac{\partial}{\partial r}\left(\frac{\phi_p}{r(p+i\omega_E)}\right) = r^2(p+i\omega_E)\left(\frac{1}{r}\frac{\partial}{\partial r}r\frac{\partial}{\partial r}-\frac{1}{r^2}\right)\phi_p - ir(r\omega_E''+3\omega_E')\phi_p\,,$$

we can integrate Eq. (2), and invert the transform to obtain

$$\phi_1(r,t) = \frac{Br}{c}\int_r^R d\rho\, e^{-i\omega_E(\rho)t}[1+i\omega_E(r)t - i\omega_E(\rho)t]h(\rho)\,, \tag{3}$$

where the initial condition is described by the function

$$h(r) = \frac{4\pi ec}{Br^3}\int_0^r d\rho\,\rho^2 n_1(\rho,0)\,.$$

Poisson's equation then gives

$$n_1(r,t) = n_1(r,0)e^{-i\omega_E(r)t} - itn_0'(r)\int_r^R d\rho\, e^{-i\omega_E(\rho)t}h(\rho)\,. \tag{4}$$

For large t, the radial integrals in Eqs. (3) and (4) are dominated by contributions from the integration limit at R, and from any stationary-phase points where $d\omega_E(r)/dr = 0$. Thus

$$\frac{c\phi_1(r,t)}{B} \sim e^{3\pi i/4}r\sqrt{t}\sum_j H(r_j-r)[\omega_E(r_j)-\omega_E(r)]e^{-i\omega_E(r_j)t}h(r_j)[2\pi/|\omega_E''(r_j)|]^{1/2} + e^{-i\omega_E(R)t}r[\omega_E(R)-\omega_E(r)]h(R) + O(t^{-1/2})\,, \tag{5}$$

and

$$n_1(r,t) \sim -e^{3\pi i/4}n_0'(r)\sqrt{t}\sum_j H(r_j-r)e^{-i\omega_E(r_j)t}h(r_j)[2\pi/|\omega_E''(r_j)|]^{1/2} + e^{-i\omega_E(R)t}\frac{h(R)}{\omega_E'(R)}n_0'(r) + O(t^{-1/2})\,, \tag{6}$$

where $H(x)$ is the Heaviside step function and the summations over j refer to the stationary points $\{r_j\}$ of ω_E. The end-point contributions correspond to the neutrally stable normal mode discussed above. The stationary-phase contributions grow secularly in time (asymptotically proportional to $t^{1/2}$, with spatial forms as shown in Fig. 1). In summary, any axisymmetric equilibrium with stationary points in the rotation frequency is unstable to arbitrarily small disturbances such that $h(r_c)\neq 0$. Asymptotically, the perturbation energy and enstrophy grow linearly in time. Our result leaves open the possibility of nonlinear instabilities in the case of equilibria where $\omega_E(r)$ is monotone, but $n_0(r)$ is not (for instance, a dense core surrounded by a thin annulus), whose stability can be spectrally indeterminate.[10]

Some unusual features of the instability should be noted. For definiteness, we consider an equilibrium such as the one shown in Fig. 1, with a single stationary point

r_c where $d\omega_E/dr$ vanishes. The density perturbation asymptotically takes the form $(dn_0/dr)H(r_c-r)e^{i\theta}$, which corresponds to a shift of the plasma core. The dipole moment associated with the dominant part of the perturbation is proportional to

$$\int_0^R dr\, r^2 n_1 \sim \int_0^{r_c} dr\, r^2 n_0'(r) \propto \int_0^{r_c} dr\, r^2 \frac{d}{dr}\frac{1}{r}\frac{d}{dr} r^2 \omega_E(r) = r_c^3 \omega_E'(r_c) = 0 , \quad (7)$$

so that the perturbation electric field near the wall does not grow. Furthermore, if a perturbation of the asymptotic form is imposed at $t=0$, then $h(r_c)$ is proportional to Eq. (7), so the amplitude will not grow. The instability is a result of phase coherence, rather than a single unstable mode.

The magnitude of the second-order mean partial flux does not increase linearly with time, in contrast to the perturbation time. The mean flux is

$$\Gamma(r) = \mathrm{Re}\, ir^{-1}\delta\phi\,\delta n^* \propto r^{-1}\mathrm{Im}\,\delta\phi(\partial^2/\partial r^2 + r^{-1}\partial/\partial r - r^{-2})\delta\phi^* .$$

Since the phase of the $O(t^{1/2})$ terms does not vary with r, the leading contribution to Γ is $O(t^{1/2})$, and oscillatory in r. The leading nonoscillatory term in Γ, which is constant in time, dominates near the origin (for smooth initial perturbations) so that the central equilibrium density increases linearly in time.

We have followed the evolution of this instability into the nonlinear stage with a two-dimensional modulated-particle-in-cell code.[11,12] We represent the density perturbation as a set of fluid elements, each of which is assigned a position $\mathbf{r}_i$ and charge q_i. The code integrates the characteristic equations for the elements, $d\mathbf{r}_i/dt = \mathbf{v}(\mathbf{r}_i)$, and $dq_i/dt = e\mathbf{v}(\mathbf{r}_i)\cdot\nabla n_0(r_i)$. The velocity field is the sum of the sheared rotation associated with the equilibrium density $n_0(r)$ and the flow due to the perturbation elements. An azimuthal spectral filter concentrated near the origin is applied to the charge density as interpolated from the particle positions onto a cylindrical polar grid. A fast Poisson solver yields the potential field. The velocity field is then interpolated back to the particle positions, which are advanced using an Adams-Bachforth scheme. The perturbation charges evolve similarly.

Some results of a typical simulation are shown in Figs. 2 and 3. We employed 32000 particles on a grid of 128 radial and 128 azimuthal points. The equilibrium is

$$n_0(r) = 1 + 2(r/0.6)^2 - 7(r/0.6)^4 + 4(r/0.6)^6$$

for $r < 0.6$, and $n_0 = 0$ for $r > 0.6$, with a conducting wall at $r=1$ (as shown in Fig. 1). This is qualitatively similar to profiles observed in a recent series of experiments.[2] The initial conditions consist of a small-amplitude $l=1$ perturbation. We measure the perturbation and its harmonics by the maximum norms of Fourier components of the grid perturbation density. The evolution of the instability and its $l=2$ harmonic is shown in Fig. 2. As a test of linearity, we show data from two runs differing only in the amplitude of the initial perturbation (by a factor of 100). Data from the smaller-amplitude case (B) are scaled for comparison in the figure. At small ampli-

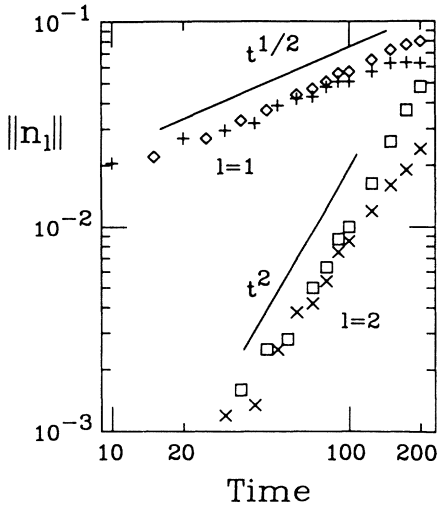

FIG. 2. Evolution of peaks of azimuthal Fourier components of the density in the particle simulation. Symbols: +, $l=1$, run A; ×, $l=2$, run A; ◇, $l=1$, run B (×100); □, $l=2$, run B (×100²). The time scale is set by the rotation frequency as shown in Fig. 1: The minimum rotation period is about 12 units.

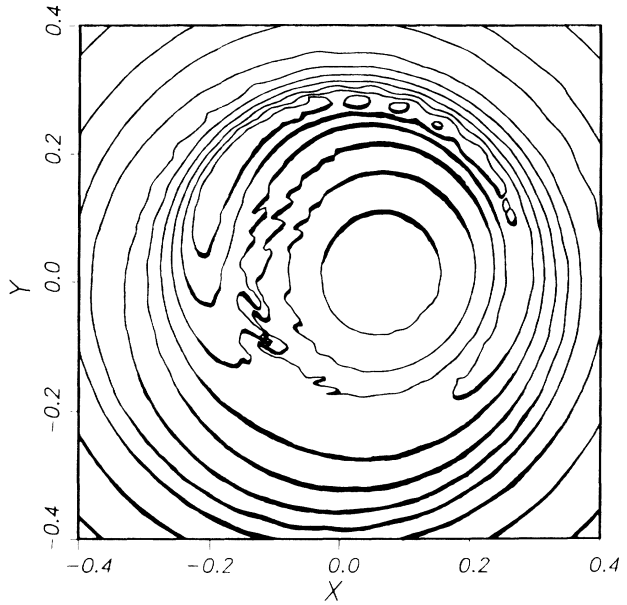

FIG. 3. Density contours of run A at $t=150$ showing sharpening of the ridge near $(x,y)=(0,0.2)$ and the secondary instability developing near $(-0.1,0)$. (Nonuniform contour intervals were used for the sake of clarity.)

tudes, the $l=1$ amplitude is described by Eq. (4) and shows a $\sqrt{t}$ trend.

The nonlinear corrections to Eq. (1) lead to several effects: rapid growth of harmonics, relaxation of the equilibrium, and secondary instabilities. The $l=2$ harmonic is driven by second-order mode coupling, and may grow algebraically or exponentially in time, depending on resonances between harmonics of $\omega_E(r_c)$ and normal modes. In the case shown, there is a near resonance involving an $l=2$ mode, which grows accordingly as t^2 for most of the run. (Numerical solution of the eigenvalue problem for the $l=2$ mode gave a growth rate of 0.0035 inverse time unit, which is negligible in the simulation.) Higher-l components grow even more rapidly. Eventually the higher-order terms can dominate the first-order ones, as in the critical layer of a Rossby wave.[13,14] In the large-amplitude run (A), the second-order mean flux eventually yields a monotonically decreasing density profile. The $l=1$ excitation saturates at a level consistent with the filling-in of the original depression.

The growing perturbation described above is subject to two kinds of localized secondary instabilities. Density contours (equilibrium plus perturbation) near the onset of secondary instabilities are shown in Fig. 3. Recall that the equilibrium density has an annular ridge. As the primary instability grows, the core shifts outwards and this ridge becomes increasingly sharp over some range of azimuths. At large times, it locally resembles a vortex sheet, which experiences a Kelvin-Helmholtz instability. Inside the saddle of the ridge, the unfavorable density gradient steepens across streamlines in a frame rotating with the perturbation. The simulation suggests that this configuration is subject to a localized instability related to those described by Haynes.[15] In cases accessible to our simulation, one or both of these phenomena occur before the low-order harmonics become large. The secondary instabilities typically involve small scales, which are not well resolved in the simulation; details of the later evolution are sensitive to the initial conditions and integration parameters.

The applicability of our description will be limited by the effects of viscosity or other dissipative processes. For the neutral fluid, an argument of Case[16] suggests that our analysis should apply to physically relevant perturbations at large Reynolds numbers for intermediate times. Moreover, viscosity would act slowly on the large spatial scales which dominate the velocity perturbation in the inviscid limit. Hence perturbations will typically show transient growth on inviscid time scales. The rapidly growing harmonics and the secondary instabilities involve smaller scales, so the nonlinear effects may be less robust. Preliminary calculations indicate that small gyroradius or viscosity in the non-neutral plasma can lead to exponential growth of $l=1$ instabilities related to the one described above, but the growth is slower than observed in experiments.[2] Dynamics along the magnetic field may also be important.

We have benefited from conversations with Dr. J. H. Malmberg, Dr. T. M. O'Neil, and Dr. C. F. Driscoll of the University of California, San Diego. This research was supported by the U.S. Office of Naval Research (N00014-82-K-0621) and National Science Foundation (PHY87-06358) (R.A.S), and by the U.S. DOE (DE-FG03-88ER-53275) (M.N.R.). The simulations were done at the San Diego Supercomputer Center, under a grant of computer time from the NSF.

[1]J. H. Malmberg, in *Non-neutral Plasma Physics,* edited by C. W. Roberson and C. F. Driscoll, AIP Conference Proceedings No. 175 (American Institute of Physics, New York, 1988), p. 72.

[2]C. F. Driscoll, preceding Letter, Phys. Rev. Lett. **64**, 645 (1990).

[3]Lord Rayleigh, *Scientific Papers* (Cambridge Univ. Press, Cambridge, 1899), Vol. 1, p. 474.

[4]V. I. Arnol'd, J. Mec. **5**, 29 (1966).

[5]R. H. Levy, Phys. Fluids **11**, 920 (1968).

[6]R. H. Levy, Phys. Fluids **8**, 1288 (1965).

[7]K. M. Case, Phys. Fluids **3**, 143 (1960).

[8]R. J. Briggs, J. D. Dougherty, and R. H. Levy, Phys. Fluids **13**, 421 (1970).

[9]M. N. Rosenbluth and A. Simon, Phys. Fluids **8**, 1300 (1965).

[10]R. C. Davidson, *Theory of Nonneutral Plasmas* (Benjamin, Reading, MA, 1974).

[11]M. Kotschenreuther, Bull. Am. Phys. Soc. **33**, 2107 (1988).

[12]N. Zabusky and J. McWilliams, Phys. Fluids **25**, 2175 (1982).

[13]K. Stewartson, Geophys. Astrophys. Fluid Dyn. **9**, 185 (1978).

[14]T. Warn and H. Warn, Stud. Appl. Math. **59**, 37 (1978).

[15]P. H. Haynes, J. Fluid Mech. **175**, 463 (1987).

[16]K. M. Case, J. Fluid Mech. **10**, 420 (1961).